

See discussions, stats, and author profiles for this publication at: <https://www.researchgate.net/publication/271467987>

# Design and analysis of an integrated 3-DOF sensor for tracking in-plane motion

Conference Paper · November 2013

DOI: 10.1109/ICCAIS.2013.6720532

CITATION

1

READS

471

5 authors, including:



**Vu Ngoc Hung**

Hanoi University of Science and Technology, Vietnam

68 PUBLICATIONS 837 CITATIONS

[SEE PROFILE](#)



**Long Quang Nguyen**

Technical University of Denmark

18 PUBLICATIONS 66 CITATIONS

[SEE PROFILE](#)



**Dzung Viet Dao**

Griffith University

357 PUBLICATIONS 4,595 CITATIONS

[SEE PROFILE](#)



**Hoang Chu**

Hanoi University of Science and Technology

60 PUBLICATIONS 255 CITATIONS

[SEE PROFILE](#)

Some of the authors of this publication are also working on these related projects:



Harsh environment thermal flow sensors [View project](#)



Chatter Detection in Milling - Intelligent Monitoring using multi sensors - PhD Thesis [View project](#)

# Design and Analysis of an Integrated 3-DOF Sensor for Tracking in-Plane Motion

Hung Ngoc Vu, Nhat Sinh Ha, Long Quang Nguyen, Dzung Viet Dao and Hoang Manh Chu

**Abstract**— In this paper, we present design and analysis of a three-degree-of-free sensor, which integrates a lateral axis tuning fork angular rate gyroscope with a two-degree-of-free accelerometer. The sensors for integrating are designed to reduce noises and improve the sensitivity by exploring mechanical couple springs. The design of the devices is carried out by simulating their mechanical behavior with the FEM method using ANSYS software and SIMULINK Matlab. The frequency difference between operation modes and parasitic ones in the gyroscope and accelerometer are 50% and 58%, respectively. The sensitivity of gyroscope and accelerometer determined from the SIMULINK model and FEM analysis are 11fF/deg./s and 11.5 fF/g, respectively. The sensors have been designed for measurement in a fully differential capacitive bridge interface using a sub-fF switched-capacitor integrator circuit.

## I. INTRODUCTION

Tracking the position of an object is an important engineering problem that finds many application areas including military, industrial, medical, and consumer applications [1 - 3]. This problem is effectively solved with an Inertial Measurement Unit (IMU). An IMU consists of three orthogonally placed accelerometers and gyroscopes, and these sensors find the linear acceleration and angular velocity of the object that it is mounted on. Knowing linear acceleration and angular velocity in three dimensions is enough to track the motion of the system with the help of additional mathematical operations [1, 2]. Compared to other sensing mechanisms, capacitive type sensing sensors have realized intensive research interest due to their advantages such as high sensitivity, high reliability, low temperature dependence, and low power consumption. The development of MEMS techniques such as bulk and surface micromachining allow to substantially improve the performance and decrease the cost of the MEMS inertial accelerometers. There are several reports on the integrated MEMS sensors. In [4], T. Sakaguchi *at.al.* presented a motion capturing system for human arm motion by integrating two types of sensor, gyroscope and accelerometer. In [5], the accelerometer was integrated in a closed-loop system, in which bandwidth, linearity and

dynamic range of the sensor was improved. In another approach, the hybrid integration was reported using CMOS circuit [6].

In this study, we present design and analysis of a three-degree-of-free sensor consisting of a 2D accelerometer and a gyroscope for an Inertial Measurement Unit (IMU). The IMU can be employed for tracking in-plane motion, in which the accelerometer and gyroscope are used for measuring two components of linear acceleration and angular velocity with the rotation axis perpendicular to the motion plane, respectively. The integrated partial sensors are modeled and analyzed using SIMULINK model and FEM analysis. The sensors have been designed for measurement in a fully differential capacitive bridge interface based on a sub-fF switched-capacitor integrator circuit.

## II. INTEGRATED 3-DOF SENSOR

In order to track the motion of an object in space, it is requisite to know linear acceleration and angular velocity in three dimensions. However, for a motion in plane, it is proper to capture a motion, when two independently linear acceleration components and angular velocity perpendicular to the plane are determined. Therefore, we here present an integrated 3-DOF sensor for measuring the mentioned acceleration and angular velocity components. Figure 1 shows schematic of the integrated 3-DOF sensor, which consists of a tuning fork angular rate gyroscope and a two degree-of-freedom. The acceleration sensor has a movable proof mass which is connected to a fixed frame via spring structures. When there is an external acceleration, the proof mass is displaced from its rest position. The magnitude of this displacement is proportional to the magnitude of the acceleration and inversely proportional to the stiffness of the

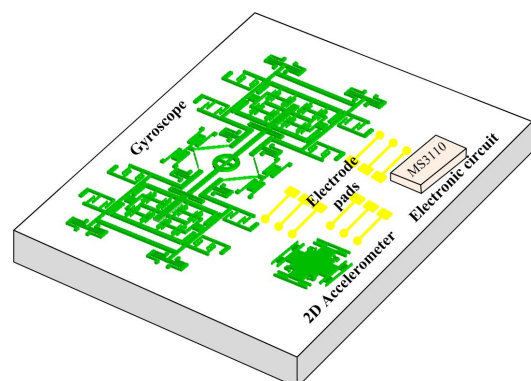


Fig. 1. Schematic of the integrated 3-DOF sensor (not in scale).

Manuscript received June 15, 2013. This work was supported in part by the Ministry of Science and Technology (MOST), Vietnam as the project of NAFOSTED coded 103.02-2010.23.

The Authors are with International Training Institute for Materials Science (ITIMS), Hanoi University of Science and Technology, No1, Dai Co Viet Street, Hai Ba Trung, Hanoi, Vietnam (corresponding authors: H. N. Vu and H. M. Chu: (+84-4-) 38680787; fax: (+84-4-) 38692963; e-mail: hungvn@itims.edu.vn, hoangcm@itims.edu.vn).

spring structures. Hence, the acceleration input that is applied to the sensor is converted to the proof mass displacement in the sensor. The sensor then extracts the magnitude of this displacement using its sensing scheme. The gyroscope is a sensor that senses external angular velocity. The similarity of the operation principle of the gyroscope with that of the accelerometer is that, the gyroscope converts the angular velocity input to displacement of its proof mass. For this purpose the gyroscope uses the Coriolis acceleration principle. First the proof mass of the gyroscope is vibrated in one axis, and then when there is an external angular velocity, the proof mass starts vibrating in another axis due to Coriolis acceleration principle. The second vibration magnitude is proportional to the angular velocity input magnitude. Hence, the sensing scheme of the gyroscope extracts the magnitude of the input angular velocity with extracting the magnitude of the secondary vibration. The sensing mechanism in the gyroscope and accelerometer is based on differential comb capacitor structure. The vibratory motion in the gyroscope is electrostatically driven by comb-drive for low power consumption. The sensors have been designed for measurement in a fully differential capacitive bridge interface using a sub-1f switched-capacitor integrator circuit (MS3110).

### III. DESIGN AND SIMULATION

#### A. Accelerometer

The capacitive-type accelerometer converts the displacement signal into the electrical signal. Figure 2 shows a schematic drawing of the accelerometer. There is a center proof mass that is anchored by four folded-beam springs. The stiffness of folded-beams is designed so that the proof mass can experience displacement in two X and Y directions, which is exerted by the inertial force causing by external acceleration. In addition, the design of folded-beams is also considered to eliminate cross-talk, which causes by mechanical coupling from parasitic vibration modes. The sense comb electrodes are arranged at the outermost edges of the center proof mass. The comb sense capacitance is split into four identical sub-capacitances,  $C_l$ ,  $C_r$ ,  $C_t$  and  $C_b$ , in a symmetrical and differential manner. The sub-capacitances form two pairs of different capacitance in X and Y directions as shown in Fig. 2. The asymmetrical comb electrode structure with two differential capacitance gaps in one pair of comb fingers is used to form the differential capacitor sense structure. When the proof mass displaces, for example to the right in X direction, the capacitances  $C_r$  and  $C_l$  will increase and decrease, respectively and inversely. The similar behavior is for  $C_t$  and  $C_b$  in the Y direction.

As shown in the design model, the principle of differential detection is employed by symmetrically placing capacitive electrodes on two opposing sides of the outermost edges of the proof mass, such that the capacitance change in the

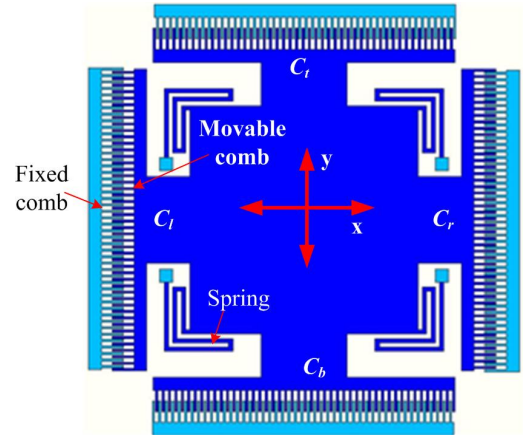


Fig. 2. Schematic of two degrees of freedom accelerometer.

electrodes are in opposite directions. It means that a differential capacitive bridge is formed. The change in capacitance for an electrode set with  $N$  fingers on each side can be calculated as:

$$\Delta C = 2N\epsilon_0 \frac{tL}{g^2} Y, \quad (1)$$

where  $t$  is the thickness of comb finger,  $L$  overlap length,  $g$  comb gap,  $Y$  the displacement of sensing electrode in motion direction.

Due to the initial value of  $g$  is  $2.5 \mu\text{m}$ , the limited value for the displacement of the sensing finger is  $2 \mu\text{m}$ . In fact, for the design of sensing capacitive structure as described above, there are two gaps, one of which is a smaller one corresponding to  $g$ , the other is larger on the opposite side. In order to optimize the large gap for the arrangement of sensing fingers, several calculations were performed. Fixing a displacement of  $1 \mu\text{m}$  in the sensing motion, a maximum large gap of  $7 \mu\text{m}$  was determined relying on the calculation of the change in capacitance  $\Delta C$  using Eq. (1). The calculated results showed that corresponding to this range the change in the capacitance is small, and even equals to zero if the distance of large gap is  $3.5 \mu\text{m}$ . Subsequently, the total gap between two adjacent fingers on one side of interdigitated capacitor set is  $12.5 \mu\text{m}$ .

In order to have a reasonable capacitance change for detecting applied acceleration, the comb fingers need made

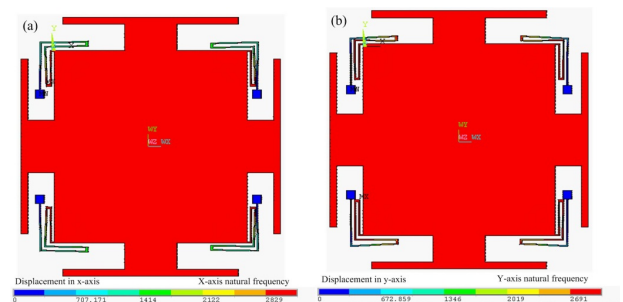


Fig. 3. The mode analysis results of accelerometer obtained by ANSYS: (a) X-mode and (b) Y-mode.

TABLE I  
FOUR LOWEST MODES OF ACCELEROMETER

Mode	Frequency (kHz)
Mode X	4.583
Mode Y	5.065
Rotation mode	7.920
Mode Z	8.606

of a thick device layer. In this study, the SOI wafer having 30 $\mu$ m thick device layer is used. By changing the dimensions of the spring beams, we model and simulate the performance of the accelerometer with the finite element method using an ANSYS software. Figure 3 shows X- and Y-mode analysis results of the accelerometer. The natural frequencies of X- and Y-mode are 4.583 kHz and 5.065 kHz, respectively. Other analysis results of the vibrating modes correspond to the higher degree modes providing frequencies greater than 7.9 kHz, which are shown in TABLE I. Thus, there is a difference of 58% between two first modes and the higher degree ones. It means that the crosstalk effect can be suppressed [7].

Based on capacitance analysis and simulation exercise, an optimized design of MEMS comb accelerometer for a balanced device sensitivity and linearity was obtained.

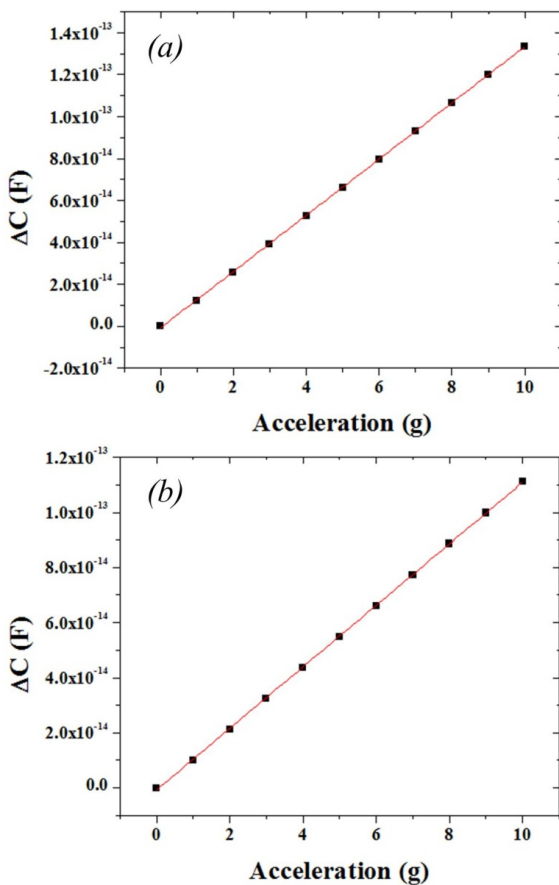


Fig. 4. Output capacitance signals simulated by FEM as function of acceleration for: (a) along X axis and (b) along Y axis.

ANSYS<sup>TM</sup> simulation shows the proposed accelerometer design has the relationship between output capacitance and acceleration as shown in Fig. 4 (a) for X-mode and Fig. 4 (b) for Y-mode. The sensitivity of designed accelerometer was estimated of about 12.5 fF/g for X-axis and 11.2 fF/g for Y-axis.

*B. Gyroscope*

Figure 5 is schematic drawing of the proposed TFG with the lateral dimension of 4500  $\mu$ m x 4350  $\mu$ m. The device is designed using Silicon-On-Insulator (SOI) wafer. The main structure of the proposed TFG design comprises two proof masses, each of which includes the outer frame (1) for driving and the inner one (2) for sensing. The drive comb electrode set (3) is attached to the outer frame (1) and designed such that in driving mode the masses oscillate in opposite direction along x-axis due to electrostatic force. The motion of comb fingers set (3) obeys the slide film mechanism providing highly stable actuation. With linear actuation of electrostatic comb force, the resonators are subjected to a harmonic motion. In this case, it is a displacement-independent force. The rotation rate is measured by capacitance change. A pair of parallel-plate sense electrode set (4) using the balanced scheme is placed symmetrically within each inner mass frame (2). This design is to increase capacitance change, i.e. the sensitivity of sensor. The dimension of comb finger is 50  $\mu$ m length and 3  $\mu$ m width. The gap between two adjacent fingers is 2.5  $\mu$ m. Upon the rotation the Coriolis force excites these mass frames in-plane motion that the differential capacitance can be detected. The design also employs the folded beams (5) for suspension. The suspensions of the proof mass are designed to allow the structure to oscillate in two orthogonal modes. The suspensions are made compliant in the drive and sense directions and stiff in other directions. The stiffness of the suspensions in the desired modes is brought close together or matched to maximize sense mode response. In our design, the width of the beam is designed to be less than the thickness. This ensures that the sense mode precedes the

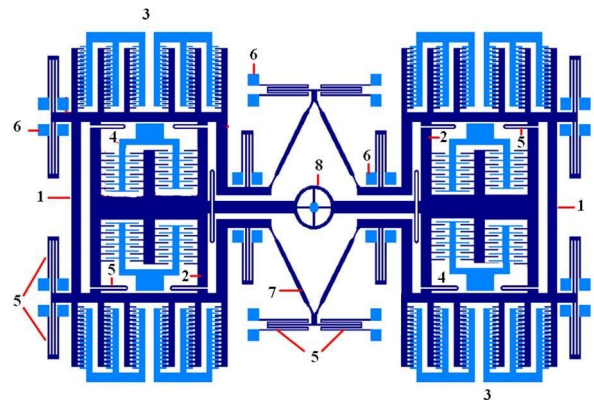


Fig. 5. Schematic of micromachined Tuning Fork gyroscope: (1) outer mass frame, (2) inner mass frame, (3) drive comb electrodes, (4) sense electrodes, (5) folded beam, (6) anchor, (7) lozenge coupling spring, and (8) self-rotation ring.



drive mode. The double folded beams (5) have the fixed ends to the substrate by anchors (6) and the other guided ones connected to the vibrating elements. Four such beams are attached to the driving mass frames allowing the expansion and contraction of the whole structure along the driving axis. The single folded beams of U-shape are utilized to join the inner frame (2) with the outer one (1) that the motion in orthogonal direction can be easily sensed.

To achieve an anti-phase oscillation in the drive-mode, the two masses are coupled with a coupling spring of the lozenge shape formed by four linear beams (7). The device is operated at the anti-phase drive frequency, which excites the masses in opposite directions as desired. In addition, the symmetrically arranged folded beams are added at four angles of the lozenge spring (7) to increase the stiffness of the whole structure. This combination is to prevent the appearance of the modes close to the driving and sensing resonant frequencies. When the sense mode response of the two masses are detected in a differential manner, their response to Coriolis forces are added, but their common-

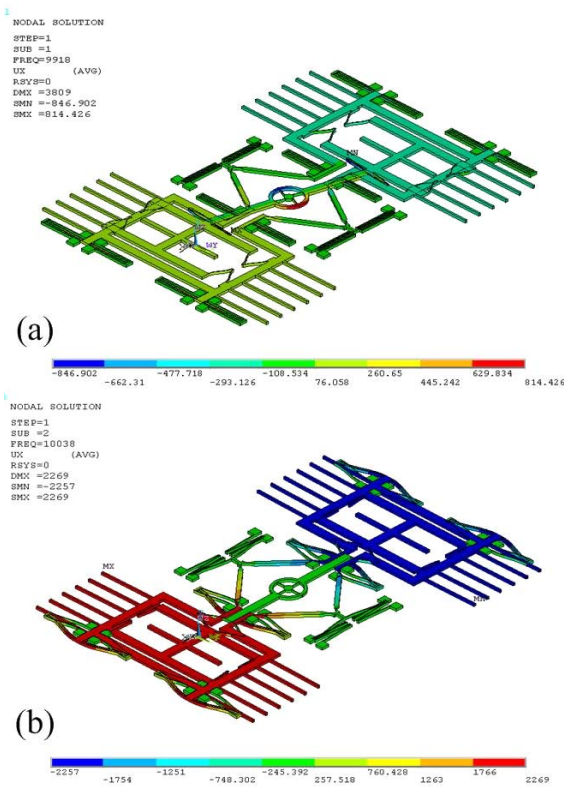


Fig. 6. FEA result of gyros obtained by ANSYS: (a) sensing mode and (b) driving mode.

TABLE II

LOWEST SIX MODES OF DESIGNED GYROSCOPE OBTAINED BY ANSYS

Mode	Frequency (Hz)
1 <sup>st</sup> (Sensing mode)	9918
2 <sup>nd</sup> (Driving mode)	10038
3 <sup>rd</sup>	14880

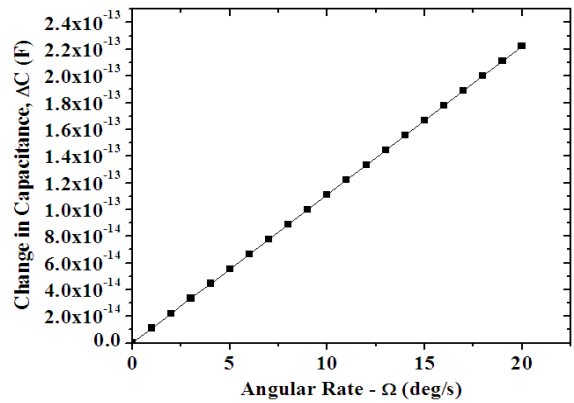


Fig. 7. Output signal simulated by MATLAB.

mode response in the same direction are canceled out. The anti-phase vibration for sensing mode is ensured by using a self-rotation ring (8).

The dimension parameters of the proof mass and the suspension beam were investigated to have the optimally designed mechanical structure of the gyroscope because vibration modes are strongly dependent on those parameters. The FEA results of sensing and driving mode are given in Fig. 6. As a result, the resonant frequencies of driving and sensing modes are determined to be 10.038 kHz and 9.918 kHz, respectively. In the fact, when the two modes are matched, the output signal is amplified by the quality factor of the sense mode, thereby increasing the sense displacements by orders of magnitude. Then, the amplitude along sensing direction achieves the maximum. However, it leads to a problem that the response time would be long. The response of the gyroscope to time varying rotation rate gives an indication of the bandwidth of the sensor. For the TFG, the larger bandwidth is attained at the cost of sensitivity. In our case, the drive and sense mode frequencies have a mismatch of about 100 Hz corresponding to the sensor bandwidth. This result satisfies the requirement to optimize sensitivity and bandwidth. Other analysis results of the vibrating modes correspond to the higher modes providing frequencies mostly greater than 14.7 kHz, which are shown in TABLE II. Thus, there is a difference of about 50% between two first modes and the higher degree ones. It means that the crosstalk effect can be suppressed.

A Laplace transform-based SIMULINK model was developed to simulate the performance of the gyroscope in the time and the frequency domain having the transient response to a given rotation rate. Based on the SIMULINK model, a dependence of the change in output capacitance on input angular rate in the range of 0 to 20 deg/s was plotted in Fig. 7. Consequently, the sensor sensitivity was determined to be 11fF/deg./s.

Theoretically, the sensitivity of the TFG is proportional to the product of sense mode quality factor  $Q_{sense}$  and drive mode quality factor  $Q_{drive}$ . Under atmospheric air condition,  $Q_{sense}$  and  $Q_{drive}$  are calculated to be 85 and 250, respectively. However, at vacuum condition of 1Pa, the

quality factors of the TFG increase up to three orders, so the sensitivity of the TFG can be improved by six orders of magnitude compared to that in atmospheric air.

#### IV. ELECTRONIC CIRCUIT FOR SENSOR SIGNAL DETECTION

The block diagram of the interface electronic circuit (MS3110) used for investigating the integrated 3-DOF sensor is shown in Fig. 8. The interface electronic circuit is a switched-capacitor integrator circuit, which consists of a charge amplifier, low-pass filter, and a buffer for amplification. It outputs a voltage that is proportional to the change in capacitance.  $C_{st1}$  and  $C_{st2}$  are the internal trimming capacitances that can be adjusted to balance the external capacitances,  $C_{s1}$  and  $C_{s2}$ . The differential capacitor pair of the acceleration sensor are connected as  $C_{s1}$  and  $C_{s2}$ , and the internal trimming capacitances  $C_{st1}$  and  $C_{st2}$  are used to balance the circuit, that is to eliminate any offset in the baseline of the voltage output. The two pairs of differential capacitors in the accelerometer and gyroscope represent for  $C_{st1}$  and  $C_{st2}$ , respectively.

When an external acceleration applies on the sensor, the capacitances of  $C_{s1}$  and  $C_{s2}$  are changed; these are reflected as the output voltage, as the bridge is no longer balanced. Charge amplifiers are used in read-out circuitry as they have the advantage of measuring very small charges thus enabling small capacitance measurement. A charge amplifier consists of an operational amplifier with a feedback capacitor (CF). The feedback capacitor has a wide range of values for selection and the selected value determines the sensitivity of the measurement. The charge amplifier is followed by a low pass filter (LPF), which filters out the high frequency components of the signal; noise tends to be high frequency. The final stage is the amplification of the signal using buffering components and amplifiers.

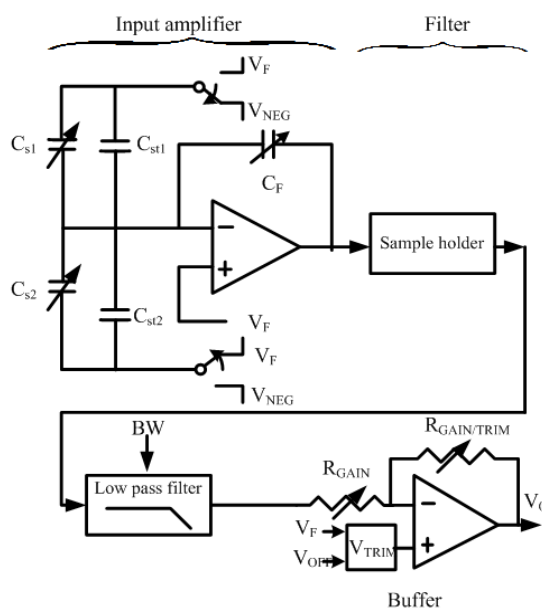


Fig. 8. Block diagram of interface electronic circuit.

#### V. DISCUSSION

From the analysis obtained in section III, there is a difference of 58% between two first modes and the higher degree ones. The frequency difference between driving and sensing mode frequencies and parasitic ones is 50%. This means that the crosstalk effect in each sensor can be suppressed [7]. In addition, as shown in TABLEs I and II the difference between the operation frequencies of gyroscope and accelerometer is 100 %, so the crosstalk causing by mechanical coupling between the sensors can be eliminated. The sensitivities of sensors were designed to be on the same order of fF. Therefore, the integration of these sensors on a single chip with a same measure electronic circuit becomes possible. The fabrication, integration and experimental investigation of the sensors are under way.

#### VI. CONCLUSION AND FUTURE WORK

We presented design and analysis of a three-degree-of-free inertial sensor consisting of a tuning fork angle rate gyroscope and a two-degree-of-free accelerometer. The mechanical behavior of each integrated sensor is analyzed by FEM method. Cross-talk in each sensor causing by mechanical coupling from parasitic vibration modes was suppressed by using properly designed suspending springs. The frequency difference between operation mode frequencies and parasitic ones in the gyroscope and accelerometer is 50% and 58%, respectively. The sensitivity of gyroscope and accelerometer determined from the SIMULINK model and FEM analysis is 11fF/deg./s and 11.5 fF/g, respectively. The sensors have been designed for measurement in a fully differential capacitive bridge interface. The differential capacitance signal is readout based on a sub-fF switched-capacitor integrator circuit (MS3110). The fabrication, integration and experimental investigation of the sensor are under way.

#### REFERENCES

- [1] M. D. Pottenger, "Design of Micromachined Inertial Sensors," *PhD. Dissertation*, Univ. of California, 2001.
- [2] S. Rajendran, K. M. Liewa, "Design and simulation of an angular rate vibrating microgyroscope," *Sens. Actuators A* 116, pp. 241–256, 2004.
- [3] Z. Qin, L. Baron and L. Birglen, "Robust design of inertial measurement units based on accelerometers," *Journal of Dynamic Systems, Measurement and Control, Transactions of the ASME* 131 (3), pp. 1-7, 2009.
- [4] T. Sakaguchi, T. Kanamori, H. Katayose, K. Sato and S. Inokuchi, "Human Motion Capture by Integrating Gyroscopes and Accelerometers," *Proceedings of the 1996 IEEE/SICE/RSJ International Conference on Multisensor Fusion and Integration for Intelligent Systems*, pp. 470-475.
- [5] M. Kraft, C. P. Lewis, and T. G. Hesketh, Closed-loop silicon accelerometers, *IEEE Pro-Circuits Syst* 146, 325, 1998.
- [6] Y. Matsumoto, M. Nishimura, M. Matsuura, M. Ishida, "Three-axis SOI capacitive accelerometer with PLL C-V converter," *Sens. Actuators A*, 75, pp. 77-85, 1999.
- [7] M. S. Weinberg, A. Kourepenis, Error sources in in-plane silicon tuningfork MEMS gyroscopes," *J. Microelectromech. Syst.* 15: 479–491, 2006.